

# INTERNATIONAL SOCIETY FOR SOIL MECHANICS AND GEOTECHNICAL ENGINEERING



*This paper was downloaded from the Online Library of the International Society for Soil Mechanics and Geotechnical Engineering (ISSMGE). The library is available here:*

<https://www.issmge.org/publications/online-library>

*This is an open-access database that archives thousands of papers published under the Auspices of the ISSMGE and maintained by the Innovation and Development Committee of ISSMGE.*

# “S” shaped curves for shallow foundations design using pressuremeter test results

N. El Khotri, M.T. Hoang, F. Cuiira, S. Burlon  
*Terrasol, Paris, France*

**ABSTRACT:** The present work is a part of the French national project ARSCOP. It aims to propose new alternatives to take into account nonlinear elastic behaviour, for the assessment of shallow foundation settlements using pressuremeter test results. New correlations between  $E$  and  $E_M$  are proposed based on the dependence of the elastic modulus according to the stress rate and the strain range. Two new approaches have been developed based on these two concepts and conventional elastic methods derived from Boussinesq's theory. They are calibrated with axial static shallow foundation tests carried out by the LCPC laboratory. Finally, the correlations and approaches thus defined are tested with the measurements related to two nuclear power plants to judge their validity.

**RÉSUMÉ :** Le présent travail s'intègre dans le cadre du projet national ARSCOP et a pour but de développer de nouvelles alternatives rendant compte d'un comportement élastique non linéaire pour le calcul du tassement des fondations superficielles avec le pressiomètre. De nouvelles corrélations entre  $E$  et  $E_M$  sont présentées pour rendre compte de la dépendance entre le module élastique et le taux de sollicitations ou de déformations. Deux nouvelles approches de calcul sont développées à partir de ces deux principes et de la théorie classique de l'élasticité de Boussinesq. Elles sont ensuite étalonnées avec des résultats expérimentaux notamment ceux réalisés par le laboratoire LCPC sur des fondations superficielles. Finalement, les corrélations et les approches ainsi définies sont évaluées au moyen des mesures relatives à deux centrales nucléaires afin de juger leur validité.

**Keywords:** Geotechnical, shallow foundations, settlement, pressuermeter.

## 1 INTRODUCTION

The assessment of shallow foundation settlement is still a major issue for geotechnical engineering as buildings and infrastructure have even more serviceability requirements. In this framework, the precision of settlement calculations needs to be improved. Two main calculation approaches are used in practice : the first approach derived from the elasticity theory and is based on the use of the equations mainly developed by Boussinesq and Steinbrenner (see for example, Terzaghi, 1943). These equations have been largely developed along the 20<sup>th</sup> century for flexible and rigid spread foundations (Giroud, 1972 and Poulos and Davis, 1974). Nevertheless, their main drawback arises from the assessment of the deformation modulus used to perform the calculation. This modulus has to be defined by considering the strain range of the ground submitted to the shallow foundation solicitation. The second approach more and more performed is based on the use of numerical modelling tools especially the finite element method. The calculation is able to provide an appropriate value of settlement for any loading level if the constitutive law used to describe the ground is well calibrated. Nevertheless, this kind of calculation is still time consuming and does not allow large parametric studies that are always useful for daily geotechnical projects.

In this framework, in order to better estimate the settlement of spread foundations, two original calculation methods have been developed to combine the variation of the deformation modulus according to the strain range and take advantage of short calculation time of analytical methods. These two methods are based on the “S” shaped curve principles: the first method (method A) is directly based on this principle since the deformation modulus varies according to the strain range while the second method (method B) is implemented by considering the stress rate level: the stiffness of the ground is decreasing when the stress state gets close to the failure criterion. The aim is to

provide the load-settlement curve of any spread foundation until a load close to 50% of its bearing capacity. For more higher loads, the time effects should be taken into account and the elasticity theory is not appropriate. The deformation modulus is assessed by considering Menard pressuremeter modulus (Ménard and Rousseau, 1962) for high strain level. These two methods are presented and compared to two sets of data: the first set is related to the IFSTTAR (former LCPC) database of full static load tests on shallow foundations and the second set concerns some measurements of two nuclear power plant buildings.

## 2 PRESENTATION OF THE METHODS

### 2.1 Principles

The two methods consider the variation of the deformation modulus  $E$  according to the strain range or the stress rate level. For the two methods, the ground under the spread foundation is divided into various layers where the deformation modulus can vary. The equation used for the two models is the same:

$$\frac{E}{E_M} = \frac{k_0}{1 + \frac{\omega}{\omega_0}}$$

where  $E_M$  is the Menard pressuremeter modulus and  $k_0$  and  $\omega_0$  are two scale parameters. The variable  $\omega$  takes into account the strain range or the stress rate level and is defined as following:

- $\omega = \varepsilon$  for the method A where  $\varepsilon$  the axial strain in the axis of the spread foundation;
- $\omega = \frac{\sigma/\sigma_u}{1-\sigma/\sigma_u}$  for the method B where  $\sigma$  is the vertical stress in the axis of the spread foundation and  $\sigma_u$  is the bearing capacity of the spread foundation (in terms of stress) (it can be assessed by any appropriate methods).

The parameter  $k_0$  shows the ratio of the deformation modulus at very low strain level to

the Menard pressuremeter modulus. Figures 1 and 2 presents the typical variations of the deformation modulus for the methods A and B (the shape of the curves will be explained later).

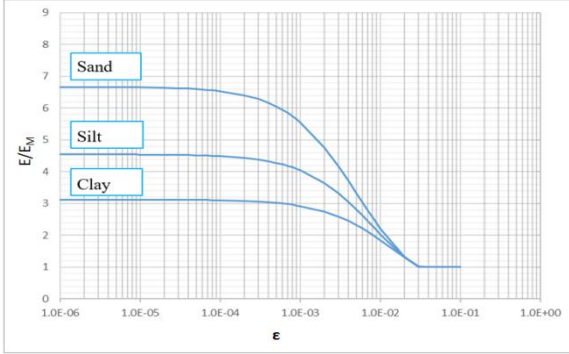


Figure 1: Elastic modulus variation according to vertical strain

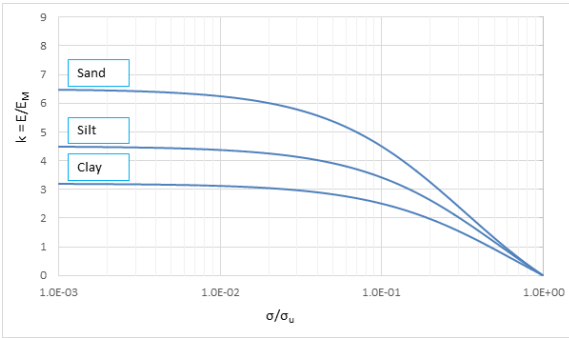


Figure 2: Elastic modulus variation according to vertical stress

## 2.2 Method A

In this method initially developed by Hoang et al. (2018), the elasticity theory developed by Boussinesq and Steinbrenner is used. Considering the layer  $i$  (with a deformation modulus  $E_i$  and a Poisson ratio  $\nu_i$ ) under the spread foundation (with a width  $B$ ), its settlement  $s_i$  is calculated by the following equation:

$$s_i = \frac{qB}{E_i} f(\bar{z}_i) \quad (1)$$

$$f(\bar{z}_i) = (1 - \nu_i^2)(F_1(z_{i+1}) - F_1(z_i)) + (1 - \nu_i - 2\nu_i^2)(F_2(z_{i+1}) - F_2(z_i)) \quad (2)$$

Where  $q$  is the load applied on the spread foundation,  $\bar{z}_i = \frac{z_i + z_{i+1}}{2}$  and  $F_1$  and  $F_2$  are two specific functions (Hoang et al., 2018).

Considering  $h_i = z_{i+1} - z_i$  and  $s_i = \varepsilon_i h_i$  in the equation (1), the following equations can be obtained:

$$s_i = \frac{\mu(z)}{k_0 E_{Mi}} \frac{1}{\left(1 - \frac{\mu(z)}{k_0 \varepsilon_0 E_{Mi} h_i}\right)} \quad (3)$$

Where  $\mu(z) = qBf(\bar{z}_i)$ ,  $k_0$  and  $\varepsilon_0$  are two parameters that must be calibrated by experimental results.

The settlement  $s$  of the shallow foundation is calculated by considering the contribution of each layer  $s_i$ .

## 2.3 Method B

In this part, we proceeded by the same way, by replacing the elastic modulus, by its expression giving by method B this time, in the Steinbrenner's formula. Considering the layer  $i$  under the spread foundation, its settlement  $s_i$  is calculated by the following equation:

$$s_i = \frac{\mu(z)}{k_0 E_{Mi}} \frac{1}{\frac{X_0(\sigma_u - \sigma)}{\sigma + X_0(\sigma_u - \sigma)}} \quad (4)$$

$$s_i = \frac{\mu(z)}{k_0 E_{Mi}} \frac{1}{\frac{X_0(k_p p_l^* - \sigma)}{qI(\bar{z}_i) + X_0(k_p p_l^* - \sigma)}} \quad (5)$$

Where  $k_0$  and  $X_0$  are two parameters that must be calibrated by experimental results. Using the pressuremeter theory for the assessment of shallow foundation bearing capacity, the term  $\sigma_u$  can be replaced by terms the terms  $k_p p_l^*$  where  $p_l^* = p_l - p_0$  is the net limit pressure ( $p_0$  is the total horizontal stress) and  $k_p$  is a parameter taking into the ground type and the foundation embeddment. The term  $\sigma$  represents the variation of the vertical stress with depth. It can be calculated for a rigid

spread foundation from the Boussinesq's theory:  $\sigma = qI(\bar{z}_i)$ . The settlement  $s$  of the shallow foundation is calculated by considering the contribution of each layer  $s_i$ .

### 3 COMPARISON WITH THE IFSTTAR SHALLOW FOUNDATION DATABASE

#### 3.1 Presentation of the database

In order to calibrate the two approaches presented below, the experimental results of 118 loading tests on shallow foundations carried out on five different sites in France (Figure 3) by the LPC network between 1978 and 1989 are used. These tests constitute a huge database that can be used for the analysis of shallow foundation behaviour submitted to vertical, inclined and eccentric loads. For this work, the results of five sites have been used to calibrate the parameters of the approaches A and B presented above. Table 1 summarizes the pressuremeter test values measured on these sites.

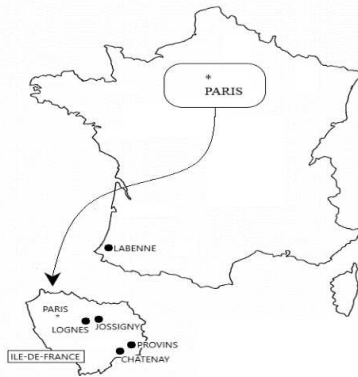


Figure 3: Localisation map of tests sites

#### 3.2 Results

For both approaches and for each type of soil the same calibration parameter  $k_0$ , which highlights that the two approaches give the same values of stiffness at small strain or small stress level. The values  $k_0$  are comparable to those measured in laboratories by means of precision tests using bender elements or resonant columns.

The results are presented by considering the calculated relative settlement (i.e., the ratio of the calculated settlement to the foundation width) and the measured relative settlement. The comparison gives sensible elements about the capabilities of the two methods A and B. Many loading levels have been considered since the measured settlements vary from 0.002B to 0.1B. Figures 4, 5, 6 and 7 provide the results of this comparison only for the sites of Labenne and Jossigny.

On Figures 4, 5, 6 and 7, each point represents the comparison between the measured and the calculated settlement for one given load level. The two blue lines plotted on these figures show the points where the ratio of the measured settlement to the calculated settlement is between 0.7 and 1.4. These two lines define a sort of confidence interval characterized by a percentage of reliability in order to precisely assess the efficiency of the two approaches.

Table 1 : Ground geotechnical properties of every site

Site	Soil	Field tests	
		$p_1^*$ [MPa]	$E_M$ [MPa]
<b>Labenne</b>	Sand	0.90	8.5
<b>Jossigny</b>	Silt	0.50	6.5
<b>Logne</b>	Stiff clay	0.75	12.0
<b>Provins</b>	Stiff clay	1.30	24.5
<b>Chatenay</b>	Chalk	1.35	19.5

##### 3.2.1 Labenne site: sand

Figures 4 and 5 present the distribution of measured and calculated settlements according to the two approaches A and B respectively. The parameter  $k_0$  is equal to 6.6 for both approaches. Suitable results are obtained in the two cases.

##### 3.2.2 Jossigny site: silt

Figures 6 and 7 present the distribution of measured and calculated settlements according to the two approaches A and B respectively. The parameter  $k_0$  is equal to 4.5 for both approaches.

Comparable results are obtained for low loads (serviceability loads), while for higher loads, method B seems more credible than method A.

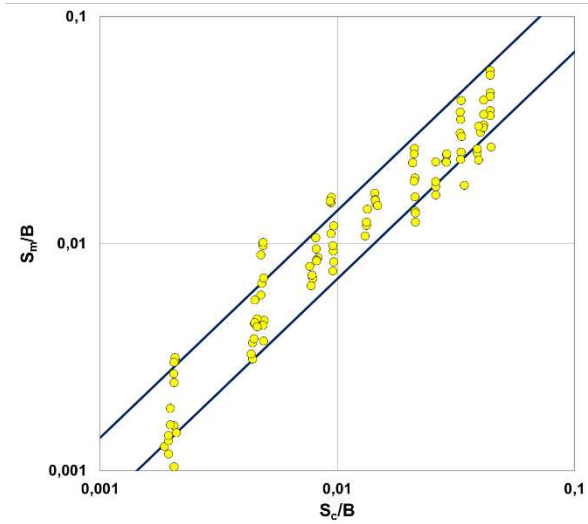


Figure 4: Measured settlement - Calculated settlement in sand - Approach A

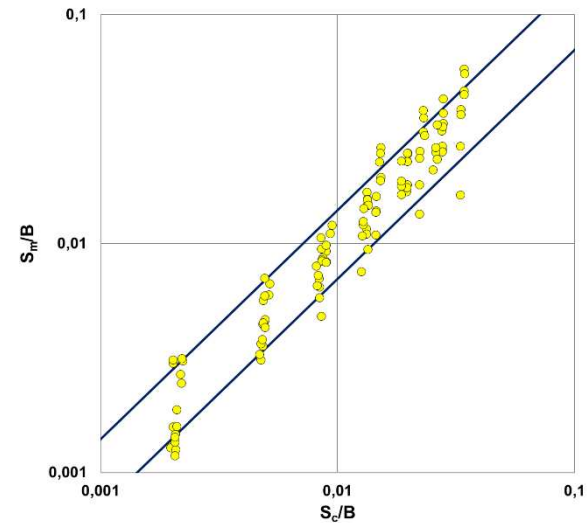


Figure 5: Measured settlement - Calculated settlement of sand - Approach B

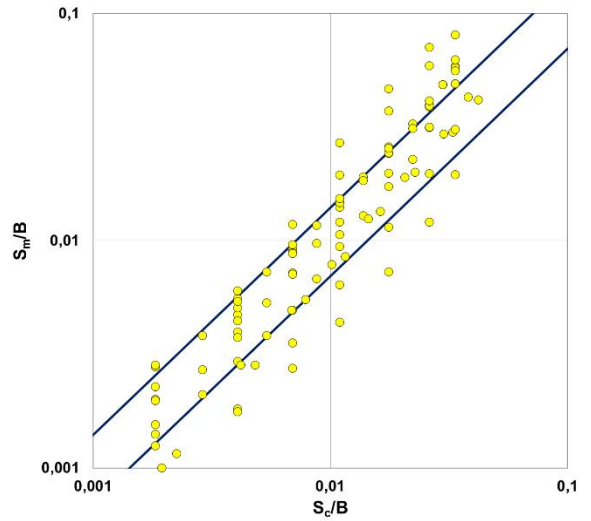


Figure 6: Measured settlement - Calculated settlement of silt - Approach A

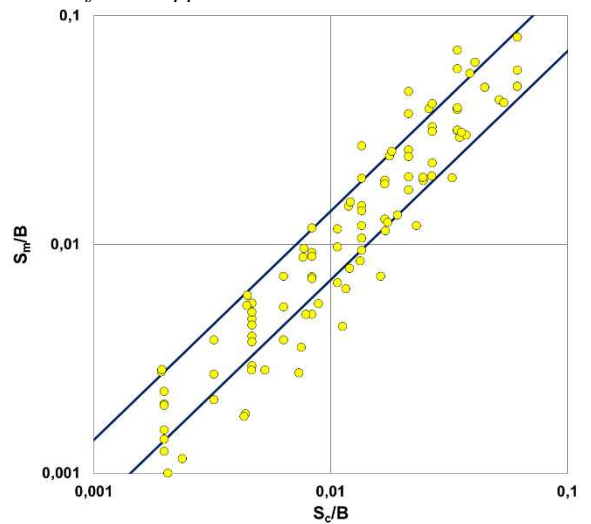


Figure 7: Measured settlement - Calculated settlement of silt - Approach B

### 3.2.3 Global Results

Table 2 summarizes the results obtained during the calibration of the two approaches A and B. The values of the parameters  $k_0$ ,  $\epsilon_0$  and  $X_0$  are provided. Moreover, for the two approaches respectively, the percentages of the points located between the two blue lines (the ratio of the measured settlement to the calculated settlement is between 0.7 and 1.4) are

given for four loading levels:  $p_i^*/3$ ,  $p_i^*/2$ ,  $2p_i^*/3$ ,  $p_i^*$ . The percentages obtained with the approach B are higher than those obtained with the approach A. This result confirms that the approach B is slightly more efficient than the approach A. Anyhow, the two methods provide very suitable results for the settlement calculation of rigid shallow foundations. They provide interesting and reliable alternatives to the conventional method proposed by Ménard and Rousseau (1962). Moreover, they have also the advantage of being exhaustively described in this paper.

Table 2: Summary table of the different results

Method A	Loading level	Calibration parameters							
		Labenne Sand		Jossigny Silt		Provins-Lognes Clay		Chatenay Chalk	
		$k_0$	$\varepsilon_0$	$k_0$	$\varepsilon_0$	$k_0$	$\varepsilon_0$	$k_0$	$\varepsilon_0$
		6.6	0.005	4.5	0.008	3.2	0.014	7	0.0047
$p_i^*/3$	63%	65%	61%	51%					
$p_i^*/2$	68%	69%	60%	52%					
$2p_i^*/3$	66%	64%	58%	46%					

Method B	Loading level	Calibration parameters							
		Labenne Sand		Jossigny Silt		Provins-Lognes Clay		Chatenay Chalk	
		$k_0$	$X_0$	$k_0$	$X_0$	$k_0$	$X_0$	$k_0$	$X_0$
		6.6	0.3	4.5	0.35	3.2	0.4	7	0.3
$p_i^*/3$	70%	70%	59%	50%					
$p_i^*/2$	74%	72%	64%	51%					
$2p_i^*/3$	76%	69%	60%	50%					

The values give the percentage of points (measured/calculated) in the range 0.7-1.4.

### 3.2.4 Typical load-settlement curves

Figures 8 and 9 present some typical load-settlement curves of rigid shallow foundations for the four sites of the LCPC database (Labenne, Jossigny, Provins and Lognes). These curves show that the two developed approaches A and B are able to account for ground non linearity. For high load levels ( $q/\sigma_u$  close to 1.0), the approach B seems more efficient. This

conclusion was expected since this approach B explicitly considers the limit bearing pressure as input data. Nevertheless, it is important to mention that for the high load levels ( $q/\sigma_u > 0.7$ ), time effects are quite significant and should be considered in the equations. For the approach A, the stiffness decrease is limited since the lowest value of the deformation modulus is equal to  $E_M$ . This approach can be mainly used for loads inducing a stress less than  $0.4\sigma_u$ .

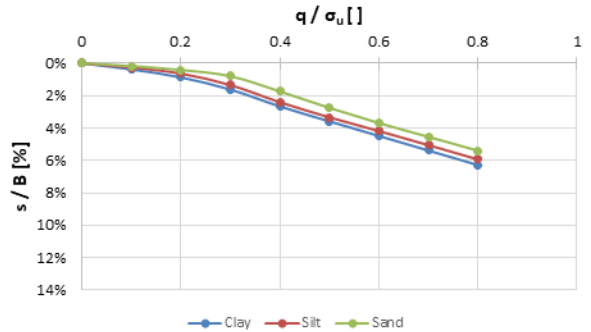


Figure 8: Typical load-settlement curves for approach A

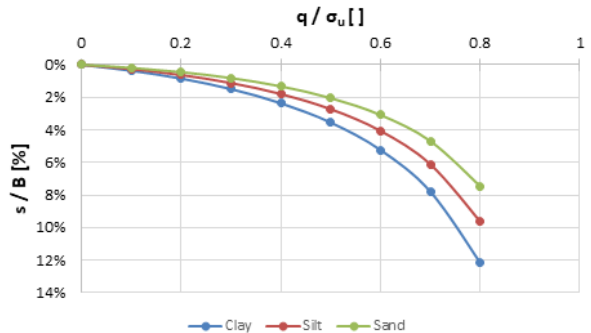


Figure 9: Typical load-settlement curves for approach B

## 4 COMPARISON WITH OTHER MEASURED SETTLEMENTS

### 4.1 Presentation of the construction site

In order to continue the validation of the two methods A and B, two other comparisons are presented based on the settlement measurements of two large buildings (118 m x 217 m in the first example and 92 m x 144 m in the second

example) of two nuclear power plants of EDF (French National Company of electricity). The geometry of the two nuclear buildings as well as the points of calculation and measurement under consideration are represented on the two following figures (Figures Figure 1010 and 11 – the points used for the comparisons are represented by some blue crosses). The stiffness of the foundation is neglected and the loads applied on the ground vary between 150 kPa and 530 kPa.

Considering the geometry of these two buildings, for both approaches, the vertical stress distribution defined by the function  $\mu(z)$  is determined according to the spatial coordinates  $(x, y, z)$ . At the location of each blue cross, the variation of this function is calculated using the Steinbrenner’s approach:  $\Delta s_i \times E_i = \mu(z)$ . In the approach B, the term  $\sigma$  is calculated by considering all the loads applied at the ground surface. All these quantities are injected in the equations (3) and (5).

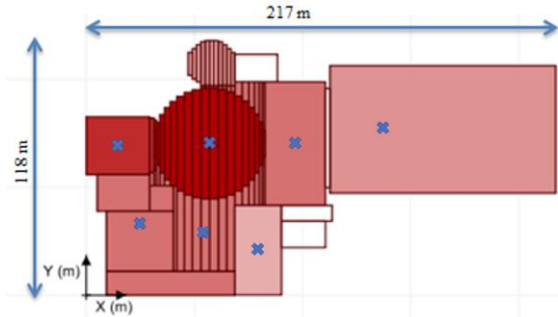


Figure 10: Model used for the raft of the first nuclear power plant

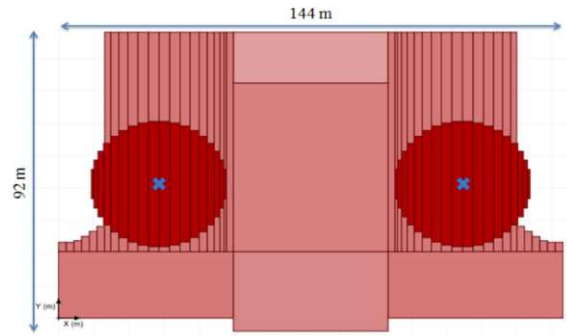


Figure 11: Model used for the raft of the second nuclear power plant

Figure 12 shows the spatial distribution of the deformation modulus using approach A for the first example. In the zones where the stresses and the strains are high, the ratio of  $E$  to  $E_M$  is 3 whereas it remains equal to 7.0 in the zones that are not submitted to high stresses and strains.

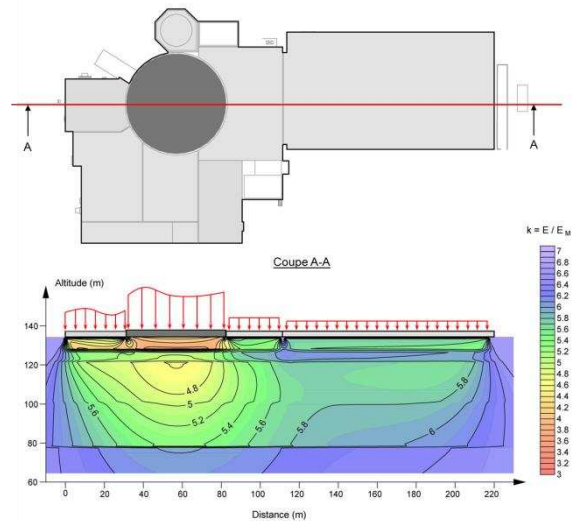


Figure 12: Spatial distribution of deformation modulus

## 4.2 Results

The results obtained for the first building plant are quite satisfactory with a maximum ratio of the calculated settlements by the two approaches to the in-situ measurements between 15% as a maximum and 3 % as a minimum. The results of the second building are less accurate. They remain credible and reliable with a



maximum difference of 17% and a minimum difference of 15%. The results obtained for these two buildings demonstrate the reliability and the robustness of the two approaches A and B for the calculation of shallow foundations and rafts settlements.

## 5 CONCLUSIONS AND PERSPECTIVES

The elastic modulus decrease with the rate of stress or the range of strain. The two approaches A and B developed in this paper are based on these concepts and aim to provide a better assessment of settlements of rigid shallow foundations and rafts (flexible shallow foundations).

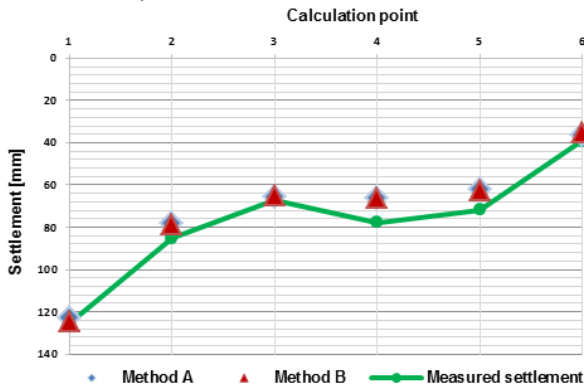


Figure 13: Calculated and measured settlements under the first nuclear power plant

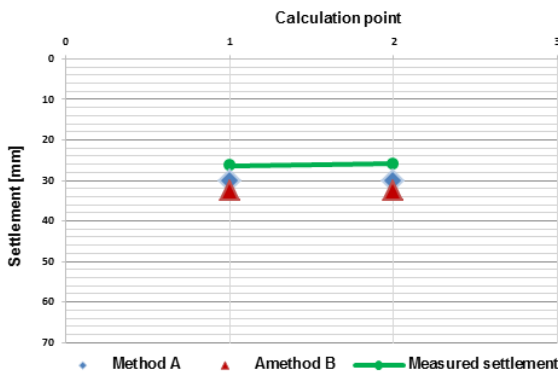


Figure 14: Calculated and measured settlements under the second nuclear power plant

In the two approaches, three parameters have been considered:  $k_0$ ,  $\varepsilon_0$  and  $X_0$ . The parameter  $k_0$  is related to each soil type and can be considered as an intrinsic parameter since it does not change by changing the calculation procedures. The other parameters  $\varepsilon_0$  and  $X_0$  take into account the range of strain and the rate of stress respectively.

For rigid foundations, the approach B that includes explicitly the value of the limit bearing pressure seems to provide better results. For flexible foundations, the approach A that includes only a variation of the deformation modulus with strain seems more appropriate.

The implementation of this kind of approaches in hybrid methods is another issue to promote. Some first calculations have been performed using the Terrasol software Tasplaq. Other application to the finite element method seems also possible.

## 6 ACKNOWLEDGMENTS

This work was prepared in the framework of the French National Project ARSCOP related to the development of a global approach for the use of pressuremeter tests for soil investigation and geotechnical design. The authors thank all the public and private partners involved in this project.

## 7 REFERENCES

- Ménard, L. and Rousseau, J. (1962). L'évaluation des tassements, Tendances Nouvelles. *Sols Soils I*, p. 13-30.
- Terzaghi, K. (1943) Theory of elastic layers and elastic wedges on a rigid base. *Theoretical Soil Mechanics*.
- Terzaghi, K. (1943) Theory of semi-infinite elastic solids. *Theoretical Soil Mechanics*.

- Giroud, J.P. (1972). Mécanique des sols. Tables pour le calcul des fondations. *Tome 1 (Tassement)*, 360 p., *Tome 2 (Tassement)*, Dunod, Paris, 1972.
- Poulos H.G and Davis E.H. (1974). Elastic solutions for soil and rock mechanics. 411 p. *John Wiley & Sons*.
- Hoang, M.T., Caira, F., Dias, D. et Miraillet, P. (2018) Estimation du rapport  $E/E_M$  : application aux radiers de grandes dimensions. *Journées Nationales de Géotechnique et de Géologie de l'Ingénieur (JNGG)*, Marne-La-Vallée, juin 2018.